A Study of Neuronal Response to Mechanical Tension

by

Jagruti J. Pattadkal

Indian Institute of Science Education and Research (IISER), Pune

Supervisors:

Dr. Pramod Pullarkat

Raman Research Institute (RRI), Bangalore

Dr. Aurnab Ghose

Indian Institute of Science Education and Research (IISER), Pune

Certificate

This is to certify that this dissertation entitled ‘A study of neuronal response to mechanical tension’ towards the partial fulfillment of the BS-MS dual degree programme at the Indian Institute of Science Education and Research (IISER), Pune represents original research carried out by Jagruti J. Pattadkal, at Raman Research Institute (RRI), Bangalore, under the joint supervision of Dr. Aurnab Ghose, Assistant Professor, Biology Division, IISER Pune and Dr. Pramod Pullarkat, Associate Profession, RRI Bangalore during the academic year 2012-2013

Dr. Aurnab Ghose
Assistant Professor
Biology division
IISER, Pune

Declaration

I hereby declare that the matter embodied in the thesis entitled ‘A study of neuronal response to mechanical tension‘ are the results of the investigations carried out by me at the Raman Research Institute (RRI), Bangalore, under the joint supervision of Dr. Aurnab Ghose, Assistant Professor, Biology Division, IISER Pune and Dr. Pramod Pullarkat, Associate Professor, RRI Bangalore and the same has not been submitted elsewhere for any other degree.

Jagruti J. Pattadkal
B.S. - M.S. dual degree student
IISER, Pune

Acknowledgements

I would like to thank my supervisors, Dr. Aurnab Ghose and Dr. Pramod Pullarkat, for guiding me through the project. I am also thankful to Seshagiri Rao, for teaching me to use the setup and his help later on. I thank other lab members of the Biophysics Lab at RRI as well, for their help during the project. Special thanks to the RRI mechanical workshop, for making and repairing the setup parts. I am grateful to RRI for hosting me for the project period and IISER Pune for the opportunity.

Cover letter:

The thesis advisory committee has recommended the thesis in its present form and no changes have been suggested and so none have been made.

Abstract:

In this study, mechanical response features of neuronal cells subjected to tension are characterized using a home-built force apparatus. We find that axons, when subjected to increasing stress in a stepwise fashion, show nonlinear viscoelastic behaviour. We propose an explanation for this behaviour based on energy release following stress dependent dissociation of cytoskeletal crosslinkers, which would result in viscous dissipation. We do not observe this behaviour for fixed cells, when comparison is done on same cell before and after fixation. This observation is in favour of our hypothesis, since the crosslinker binding in fixed cells will be covalent. We are further testing the hypothesis by developing a model based on it, the predictions of which will be tested experimentally. Other response features studied include the axonal tension and net elastic constant, their variation with strain. Both are found to decrease with strain. Thus, we observe live axons to show strain weakening response when subjected to increasing stretch. The work establishes the use of a novel optical fibre based force apparatus for quantitative measurements on axons, which can be used in future to address diverse problems in axonal mechanics.

List of figures

List of tables:

1. Introduction:

Interaction with the physical environment is inevitable for a neuron, or for that matter for any other cell. Different physical forces in the environment will have an effect on the cells depending on cell's susceptibility to these forces. By virtue of it being a material, a cell would be affected by mechanical forces; the effect based on cell's sensitivity. A cell may then use these readily available mechanical stimuli as cues related to its survival and functioning. The importance of mechanical forces in development and functioning of tissues, though not so well studied till recently, has been proposed since a long time back (D'Arcy Thompson's 'On Growth and form', 1917). An increasing number of studies in the recent years, are showing evidence for physical stimuli to be as influential as the well-studied chemical factors, in cell's development and function. For example: Mechanical tension can have significant effects on cell cycle progression (Huang et al, 1998), cell growth and cell fate switching (as reviewed in Mammoto et al, 2009). Cell stretching induced tension has been shown to affect behaviour such as invasive cell migration in *Drosophila* (Somogyi et al, 2004). Mechanical forces generated at the cell surface receptors can bring about changes in gene expression inside the nucleus (Wang et al, 2009). Force such as the fluid shear stress can inhibit cell proliferation in certain cancer cells (Avvisato et al, 2007), can bring about activation of secondary messengers and, over long time, changes in gene expression (Davies and Tripathi, 1993). Mechanical stimuli can also affect protein synthesis rates, a plausible mechanism for exercise based increase in muscle mass (Hornberger and Esser, 2004), and also protein states (Nicklas et al, 1995). An important source which imposes mechanical stimuli on cells is the extra-cellular matrix (ECM) and its stiffness is also known to affect cell contractility and proliferation and can contribute to tumour formation (Huang and Ingber, 2005). Neurons are also sensitive to substrate stiffness (Franze et al, 2009). Forces generated inside the cell can also affect functioning of other components, for e.g.: tension states in fibroblast regulate the necessity of microtubules for dendritic process formation (Rhee et al, 2007), adhesion associated cell shape and cytoskeletal tension changes are necessary for downstream activation of ROCK (Bhadriraju et al, 2007). Other than mediating effects through these conventional signal transduction pathways, physical forces can also bring about changes by rapid mechanotransduction, mediated by a prestressed cytoskeletal network (Hwang et al,

2012). A cell's response to any cue and its functioning, as shown by these and other examples, would then be a resultant of interaction of biochemical pathways, cytoskeleton and membrane structures and the physical forces acting upon them.

We are studying the effect of mechanical tension on neurons. These cells are very unique in their morphology. Their axonal processes can range from a few micrometers to a metre in humans, while maintaining a diameter of only around a micron. This peculiar aspect ratio presents its own challenges for neuron functioning. Conducting stimuli, forming networks, maintaining their structure and also allowing plasticity, bringing about damage repair at such length scales would impose special demands on the axonal cytoskeleton and membrane. Mechanical signal transduction, known to be faster than the reaction diffusion type transductions (Na et al, 2008), may also offer special advantages to neurons at their length scales.

1.1 Axon structure:

One of the factors deciding the neuronal response to mechanical tension is the mechanical property of the neuron itself. This is decided by its structure. To describe the axonal structure in short, it is a thin membrane tube whose interior is packed with the cytoskeletal elements and associated proteins. Cargo travels along these cytoskeletal tracks. There are three main cytoskeletal elements: the microtubules, the intermediate filaments known as neurofilaments, and the actin filaments. The microtubules with their persistence length of few hundred microns to few mm, behave as rigid rods. The neurofilaments are flexible with persistence length of only around a micron. They thus provide resistance against mechanical stress. The actin filaments, with persistence length of around 10 microns, are semiflexible polymers. The cytoskeleton is able to couple itself to the extracellular environment by interacting with the transmembrane proteins which themselves interact with the extracellular cues.

1.2 Overview of known neuronal functional responses to tension:

Some of the known effects of mechanical tension are described below:

1. Effect on growth:

   There are two phases of neuronal growth, as reviewed by Franze and Guck,

2010. An initial phase is driven by the growth cone motion during network formation. Directional forces are generated inside the growth cone, based on the extracellular physical and chemical cues. Growth cone force then pulls the associated neurite, thus generating tension and causing growth. The second phase of neuronal growth is caused by network expansion. Axons already connected are stretched in this case. Thus, mechanical tension plays an important role in both these growth phases.

Evidence that growth cone can indeed pull was provided by Lamoureux et al, 1989. An increase in tension accompanying growth cone advance was observed in this case. Towed growth, or growth along the length of the axon mediated by tension, was suggested by Harrison in 1935 and P. Weiss in 1941 (ref. in Bray. 1984). Bray 1984, first showed that mechanical tension itself could act as a cue for neurite growth. Using a microelectrode to pull the growth cone, he observed that the axon could grow (based on neuronal volume increase) at medium pull rates (100 micrometer/hr or less). However, they failed to grow at higher rates, though the elasticity was maintained. Experiments by the Heidemann group (eg: Zheng et al, 1991) on towed growth, showed that the axonal elongation rate was linearly related to the tension level in the axons of peripheral neurons, for tension above threshold. At a given tension, the neurite would continue to grow instead of equilibrating (Dennerll et al, 1989). Axonal growth following tension requires addition of new mass. A study on this mass addition, by Lamoureux et al 2009, showed that volume increase, following tension induced viscoelastic stretching of the axon, occurs by intercalated addition of material.

Growth of integrated axons under extreme stretch rates was studied by Pfister et al, 2004. They subjected axons to stretch rates of upto 8 mm/day and, rather remarkably, the axons were able to elongate at these rates while maintaining their caliber, organization of internal elements and functional ability as well (Pfister et al, 2006).

Another notable effect of tension is the neurite extension from cell body upon

pulling at the cell surface. This is found to be a neuron specific effect (studies referred in Heidemann et al, 1995). Reports suggest a preferred force range for this neurite initiation (Fass and Odde, 2003) and neurite subjected to constant force is found to elongate at variable instantaneous rates.

2. Effect on cell and network structure:

   Tension can affect neuronal morphology, for eg: by causing axonal specification for hippocampal neurons. Here, of the multiple neurites from a cell body, the one which first exceeds the threshold tension and starts elongating at a rapid rate becomes the axon (Lamoureux et al, 2002). Tension can also affect network structure. Equilibrium of tension and other adhesive forces can explain neuronal branching pattern (Bray, 1979, Shefi et al, 2004) and a resultant tension force can also guide neuronal cell migration (Hanein et al, 2011) . Tension dependent branch stabilization also affects network development (Anava et al, 2009).

3. In vivo effects:

   In addition to above mentioned in vitro studies, in vivo studies are also conducted to test if neuronal development in vivo is affected by tension as well. Rajagopalan et al, 2010, based on their studies in *drosophila,* show that in vivo axons also have a rest tension, behave viscoelastically and actively regulate tension levels. In vivo branching pattern is also regulated by tension, as shown by Condron and Zin, 1997, for a particular node of a local serotonergic interneuron in a grasshopper embryo. Transecting one of these branches would cause snapping of the network geometry. Mechanical tension is required for vesicle clustering in vivo in *Drosophila* neuromuscular junction (Siechen et al, 2009). These neurons were also shown to maintain a rest tension and restore it if perturbed. Similar result is reported by Ahmed et al, 2012, where they show global accumulation of synaptic vesicles at drosophila NMJ, in response to tension, using live cell imaging. A study by Paulus et al, 2009, shows that muscle contractions in zebrafish are necessary for in vivo axonal guidance of Rohon-Beard neurons - a class of peripheral neurons.

1.3 Overview of neuronal mechanical responses to tension:

Most biological materials, when exposed to stress, show a viscoelastic behaviour. This is a combination of elastic and a viscous response. For a elastic response, stress (σ) is proportional to strain (ε) and the proportionality constant is the Young's modulus (E).

$\sigma = E\varepsilon$

For a viscous response, stress is proportional to strain rate and the proportionality constant is the viscosity (η). $\sigma = \eta\frac{d\varepsilon}{dt}$

Thus, the strain response of a viscoelastic object, when subjected to stress, will evolve over time. When neurons are mechanically pulled, their response varies depending on the timescale and the force thresholds. Dennerll et al, 1989, based on their studies on PC12 and chick DRG neurons, suggested that neuron elongation in response to tension is a three way control. Below a certain threshold, the cells actively generate tension thus shortening neurite. Above a certain threshold, the neuron actually grows (towed growth). Between these two thresholds, the neurite responds as a passive viscoelastic object. The model used for description of this viscoelastic object is shown in the figure 1A. Similar study on chick forebrain neurons (Chada et al, 1997), showed them to be less elastic in nature compared to chick DRG neurons. The response of forebrain neurons was dominated by viscous component and thus closer to a viscoelastic fluid. Also, these neurons did not show any sign of active contraction, observed in DRG neurons.

Neuronal response to tension also varies based on the timescale, as shown by Bernal et al, 2007 in PC12 neurites. A fast response of axons to tension was shown to be viscoelastic, and active contraction was observed over intermediate time period. The model proposed in this study is shown in figure 1B. Active component is suggested by Dennerll et al, 1989 as well, as a cause for regaining of tension, following tension release, which cannot be explained by any viscoelastic model. Mechanical pulling studies in axon also indicate existence of rest tension, inferred from elastic response of axons to rapid plucking (Dennerll et al,1988).

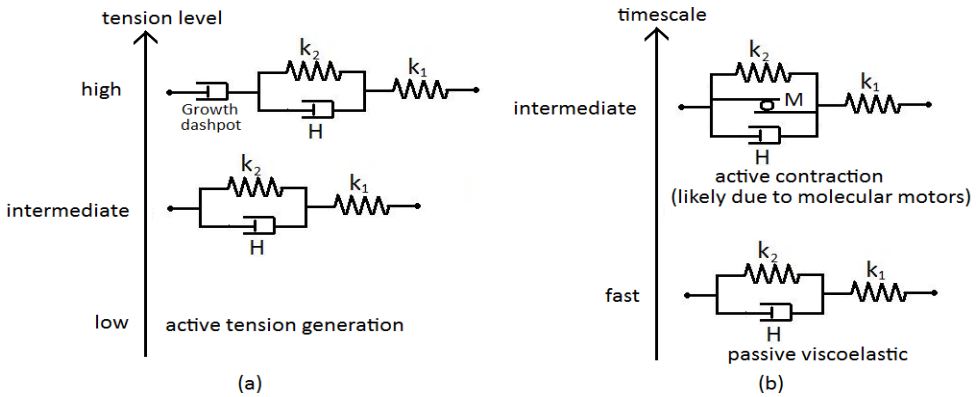

Figure 1: Models suggested for axonal mechanical response:
(a) Model by Dennerll et al, 1989; (b) Model by Bernal et al, 2007, adding a motor element to explain active contraction observed at intermediate time scales.

1.4 Techniques for studying neuronal response to tension:

Various methods have been used so far to study the neuronal responses to mechanical tension. One of the oldest attempts to deform the axon and measure the force was by Sato et al, 1984. This group has used a magnetic sphere viscoelastometer. It consists of injecting magnetic beads inside the axon and then imposing force on the bead and hence the axon, using magnets. This was the first study to show that axon behaves as a viscoelastic object. Bray, 1984, using a cell puller,based on electric motor and a glass microelectrode to pull neurons. Heidemann's group used calibrated glass microneedles driven by micromanipulators (eg: Zheng et al, 1991), advantage being, the force could also be measured. Fass and Odde 2003, for their studies on tension based neurite initiation, have used integrin antibody coated magnetic beads, which can be moved by electromagnets. The current in the coil and the stage position is used to manipulate the force. Another system which can measure forces is by Bernal et al, 2007. Their group has again used calibrated glass needles, driven by precision DC motors. Bernal et al 2010, have also used laminar flow to impose drag force on PC12 neurites and measure the mechanical response. Mechanical stress imposition in Franze et al, 2009 is done using beaded cantilever and SFM. Tang-schomer et al, 2010 have used a micropatterned silicon membrane substrate placed on a chamber where air pressure can be varied, for conducting dynamic stretching experiments. This was used to assess damage response of the cytoskeleton. Siechen et al, 2009 and Rajagopalan et al,

2010, for their in vivo studies in *Drosophila*, have used micromechanical force sensors, which consist of a probe and a reference beam and are driven by a piezo actuator. Some examples of systems which can induce stretch but cannot measure force include a custom made expansion chamber driven by microstepper motors used by Pfister et al, 2004, a silicon membrane based cell stretcher used by Chetta et al, 2010, and a PDMS based cell stretcher used by Ahmed et al, 2012.

1.5 Scope of current work:

In this study, we are interested in assessing neuronal response to tension using a novel home-built force apparatus (PhD thesis S. Rao, to be submitted, patent pending) . This device uses an optic fibre to induce tension in the axon and force is measured based on fibre deflection. Being coupled to a microscope, the device allows a thorough characterization of mechanical response of axons and we are beginning to do this characterization. Some advantages of this system are its high piezo range, allowing axons to be stretched upto 90 microns; possibility of conducting measurements imposing different constraints on the sample, such as constant force based, constant strain based or oscillatory mode; large range in the force resolution starting from picoN to microN level; possibility of coupling to fluorescence or confocal imaging which can be used to probe the cell mechanisms behind its responses to tension. Results of this axonal mechanical response characterization experiments are presented in this report.

2. Materials and methods:

1. Cell culture:

   Dorsal root ganglion neurons from 8-9 day old chick (*Gallus gallus*) embryos are used. The ganglia are dissected from the embryos and trypsinized in 0.25% trypsin. The cells are then plated in L-15 medium (Gibco 111415) containing methocel E4M (Colorcon ID 34516) at 6 mg/ml,10% FBS (Gibco 10100) and D-glucose (Sigma G6152) at 6 mg/ml. NGF (Invitrogen 13290-010) is added to this medium at 20 ng/ml. Antibiotic PSG (Invitrogen 10378-016) is also used at 05 mg/ml concentration. The culture surface is a thoroughly cleaned glass coverslip with no further protein or other coatings. On this a glass ring of inner

diameter 14 mm and height 1 cm is stuck using vacuum grease. The cultures are incubated at 37°C, atleast overnight before use. Before the sample is used, since the methocel containing medium is viscous, the medium in cultures is replaced, before the experiment, with L-15 medium with all the same constituents as above, except the methocel. NGF and antibiotic are also not added. After replacing the medium, the sample is again left for incubation for 30-60 min, so that cells recover.

2. Setup:

   The idea of the setup is to use an etched optic fibre as a force transducer. The deflection of the cantilever is measured to get the force readout. The optic fibre is used to impose force on the axon. When the cantilever deflects by δ, the force will be $F = k \times \delta$, based on Hooke's law.

   The schematic of the setup is shown in figure 2. The setup is built on a microscope (Zeiss Axio Observer D1). Laser light (Melles Griot 25 LHR-925-230, He-Ne laser) is passed through the optic fibre (THORLABS). The laser light is collected using a position sensitive detector (Hamamatsu photonics, PSD 2044). The fibre is loaded on an in-house designed brass cantilever holder. The holder is loaded on a piezo (Physik Instruments P-841.60). The piezo is mounted on an in-house designed aluminium stage. Camera (Andor Luca EMCCD) is used for acquisition at 1 or 2 fps. The whole setup sits on a vibration isolation table. The software code for reading the PSD output and controlling the piezo was developed in labview as a part of this project.

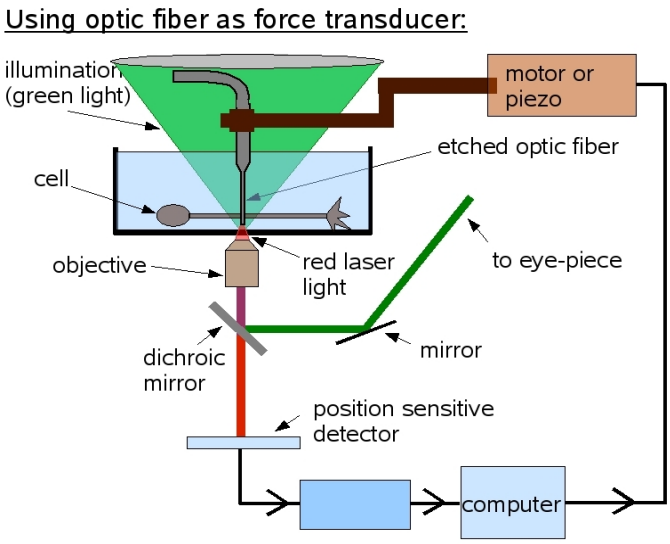

Figure 2: Schematic of the force apparatus (S. Rao Ph.D thesis to be submitted) used for pulling axons

3. Preparing the cantilever:

The optic fibre comes with a plastic sheath around it. The sheath is covered further by another jacket. The fibre diameter is originally 120 microns. The fibre is first loaded on the cantilever holder. Before etching, the outer sheath is cut and the inner sheath is burnt. The assembly is then etched in 48% hydrofluoric acid with stirring. The fibre stiffness depends on its dimensions. There is a constraint on the length of the fibre, since the sample well height is 1 cm. So, the fibre length is usually kept at 7mm. Then, to get the stiffness in the right range, the fibre is etched till it attains a diameter around 15 – 20 microns (70-90 min). The fibre is then washed with water. Next, the cantilever holder is glued at the base of the fibre using an adhesive (fevikwik). The other end of the holder is also glued for more stability. The stiffness of the fibre is measured based on its dimensions. For this, resonance frequency calibrations in air, done previously, are used. The details of the calibration setup and verification procedure will be presented in following reference (Ph.D thesis S. Rao). Briefly, the characteristic frequency of the fibre is linked to its Young's modulus and the moment of inertia, by the following equation:

$$\omega = \frac{3.516}{4}\sqrt{\frac{EI}{\rho s}},$$

where E = Young's modulus of the cantilever material, I = area inertia of the rod, S =cross-section area of the rod, ρ = density = 2.297 $\times 10^3$ kg/m^3.

d = fibre diameter, l = length of the fibre

Substituting the formula for area inertia for cylindrical rod, $I = \pi d^4/64$ and $S = \pi d^2/4$, the equation becomes:

$$\omega = \frac{3.516}{4}\sqrt{\frac{E}{\rho}\frac{d}{l^2}}$$

Based on calibration plots for ω vs (d/l^2), value for E is obtained.

The spring constant of the cantilever is then:

$$k = 8.5 \times 10^{(-5)}\frac{d^4}{l^3}$$

The diameter of the fibre is measured using the camera. Substituting the values in the above equation, k of the cantilever is found.

4. Noise elimination:

Initially, when the PSD data was collected, after dipping the cantilever in medium, the noise range was large (> 1micron std. deviation) (figure 3A) . In order to minimize this noise, we covered the sample surface with oil. This would reduce the heat exchange due to temperature difference between the sample surface and the surrounding, in turn minimizing noise due to convection currents. This reduced the noise to a significant extent (0.3 micron std. deviation) (figure 3B) . However, occasional spikes were still present in the data. We then decided to cover the assembly on Al -stage with a chamber. This would reduce the disturbances due to external influences, such as air currents. This reduced the noise to a very low level, with the deviation comparable to the highest resolution of the system capturing the light (35 nm) (figure 3C).

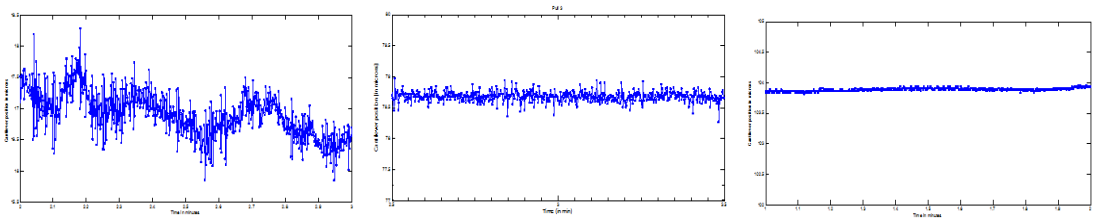

Figure 3: Noise elimination in PSD reading

Plots of PSD displacement vs time. (a) PSD reading indicating initial noise level, (b) PSD reading after covering sample surface with oil, (c) PSD reading after

covering the assembly on stage with a chamber. The x (1 min) and y (3 microns) range of all three plots is equal

5. Using the setup:

   The sample well is placed on stage. The etched fibre acts as a cantilever. It is dipped inside the sample, till the whole of its length is inside the medium. The x, y and z position of the cantilever can be controlled by manually moving the screws on the piezo holder. The surface of sample, after dipping the cantilever, is covered with oil, to reduce convection currents. The sample well is moved manually to find an axon and orient it for the pull. The cantilever is then brought in touch with the axon using the x, y, z, screws. The laser intensity of the spot coming out of the fibre is adjusted at an optimum for the PSD (2.5 – 3.5 V). The cantilever is then moved using the piezo. An initial trial is done to see if the axon can be pulled. Then the axon is brought back to its relaxed state and the desired experiment is conducted using Labview codes. The movement for the piezo and the PSD acquisition (10 Hz) can be programmed through labview. Before recording, the stage is covered with an aluminium chamber, to minimize external disturbances. The experiments are conducted at room temperature, and no sample is used for live measurements after 2.5 – 3 hrs on stage.

6. Experimental scheme:

   At the start of the experiment the tip if the fiber is placed in contact with an axon at approximately its mid point. Care is taken to ensure that the fiber is not touching the glass surface. From this point of time, the computer records the PSD position (zero force) and controls the piezo. For the multiple step pull protocol, the piezo is given a command to move by a fixed step after a fixed time interval (figure 4). The PSD keeps recording the temporal evolution of the force and strain. The camera separately collects images during this run. Images are collected at 40X.

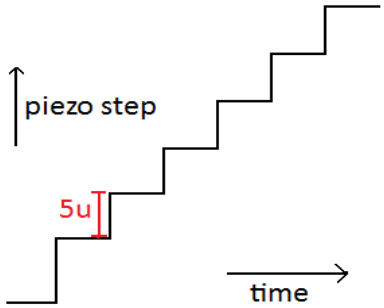

Figure 4: Schematic of the piezo movement for the multiple step protocol
The piezo is moved in fixed steps (5 microns) at fixed time intervals (150 s).

7. Fixation:

   For fixation of the sample on stage, the medium inside the well is first removed as much as possible. Then, fixative is added to the well. The fixative composition is 5% glutaraldehyde + 3.2% paraformaldehyde in 1X PHEM buffer. The sample undergoes fixation for atleast 20 min before conducting experiment. The fixative stays in the sample well even during the experiment (for next 1 – 2 hrs).

8. Analysis:

   The image analysis is done using ImageJ. Length measurements are converted from pixels to microns based on the calibrations for the camera (1 pixel = 0.194 microns, at 40X for ANDOR). Further analysis on the collected data is done in Matlab. (see figure 5)

   The program output includes the x and y coordinates of the laser light, tracked over time. This corresponds to the tip position of the cantilever. The piezo position (D) over time is also obtained simultaneously.

   Based on the x and y coordinates of the laser, the cantilever displacement (d) is calculated as: $d = \sqrt{x^2 + y^2}$

   For the stepped pull protocol, the piezo is given a fixed step (D). The cantilever displacement is tracked over time.

   Deflection in the cantilever is then $\delta = D - d$

   So, the force experienced by the cantilever $F_c = k_c \times \delta$

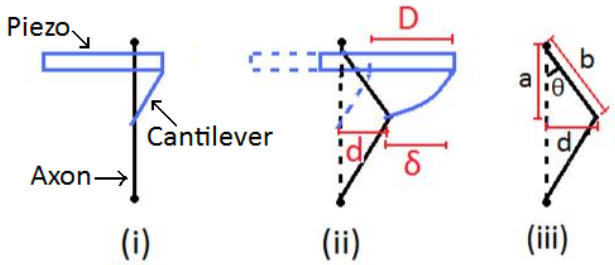

Figure 5: Schematic of the axon pull

Blue bar represents the piezo. Blue line is the cantilever, perpendicular to the sample surface. (i) The cantilever in touch with the axon before pull, (ii) The axon is pulled in transverse direction, (iii) The variables used for analysis are marked in the figure.

This force is equal to the component of tension in the opposite direction. Let tension in the axon be T. So, $2Tsin\theta = F_c$

Since, $sin\theta = \frac{d}{b}$; $T = F_c/2sin\theta = bF_c/2d$

If the measured length of the axon at time t is $L(t), b(t) = L(t)/2$

So, tension in the axon can be estimated as

$T(t) = F_c(t)b(t)/2d(t) = F_c(t)L(t)/4d(t)$

The length of the axon is obtained by measuring the length in the captured frames. Since the frame number is large, instead of measuring the length in every frame, only representative frames captured during the response phase being studied (for eg: immediately after pull or after relaxation) are used. The axonal strain is obtained by subtracting the initial axon length from the lengths measured after the pulls. The relative strain in the axon is measured as the strain divided by the initial axon length.

To obtain the net elastic constant (K), force of the cantilever, after viscous relaxation, is measured by averaging the last but 100 values. The cantilever displacement value after relaxation is obtained in same manner. The length of the axon is obtained by measuring the length in the frame captured just prior to the next piezo step. Based on these force, cantilever displacement and axon length measurements, tension in the axon after relaxation for every step is

calculated. The strain is obtained by subtracting the initial axon length from the lengths measured for every step, after relaxation. The total elastic constant is then equal to $K = \frac{axonal\ tension\ after\ relaxation}{axonal\ strain\ after\ relaxation}$

Figure 6 below shows images of the experiment.

a) before pull

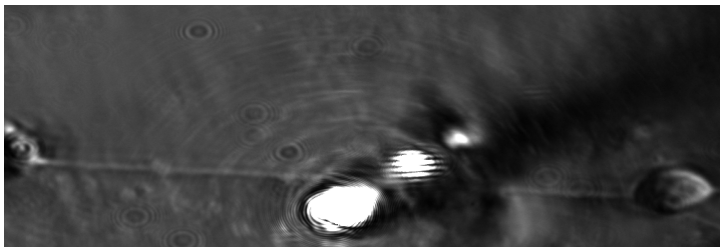

b) after pull

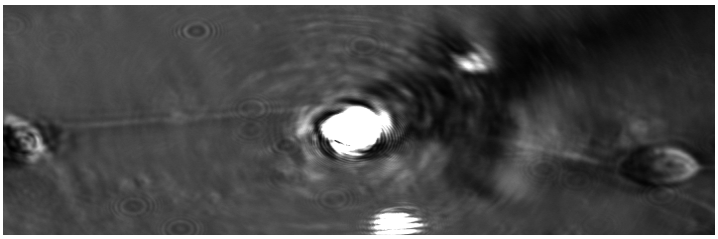

Figure 6: Images of axon being pulled

(a) Axon before pulling. The bright spot is the cantilever tip, (b) Axon after pull.

3. Results and discussion:

Most biological materials are viscoelastic. To be able to understand and predict the behaviour of viscoelastic objects, they are often modeled as combinations of elastic (spring) and viscous (dashpot) objects (mean field approach). Model predictions are then fitted to the experimental values to test their validity, whereupon the model may be improved or used to generate predictions. Two of the most simplistic models use a combination of a spring and a dashpot, either in series (Maxwell model - figure 7i) or in parallel (Kelvin - Voigt model - figure 7ii).

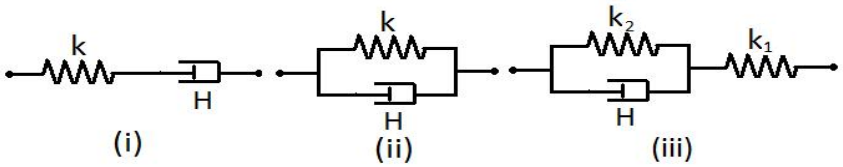

Figure 7: Models of viscoelastic objects.

(i) Maxwell model, (ii) Kelvin-Voigt model and (iii) Model used for axon

When subjected to sudden step stress, a Maxwell material, being a viscoelastic fluid, will show an elastic jump, followed by change in strain, which increases linearly with time. When subjected to sudden step strain, the Maxwell material will show an exponential relaxation in stress. Likewise, for a Kelvin-Voigt material, when subjected to sudden stress, the strain will increase at a decreasing rate with time finally reaching a steady state. This behaviour is also known as creep. The viscoelastic response of the axon, when pulled, shows an initial elastic jump, followed by a strain relaxation (see figure 8). So, an approximate model for axon behaviour is made by adding a spring in series to a Kelvin-Voigt element (as in Dennerll et al, 1988) as shown in figure 7(iii).

a) b)

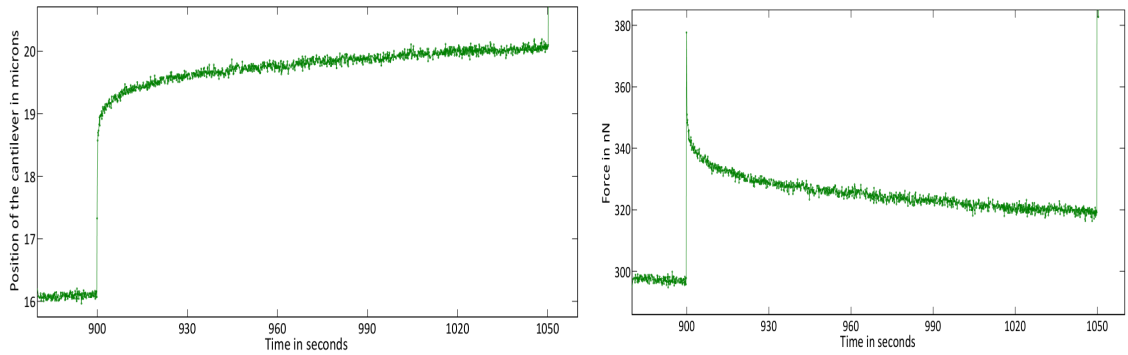

Figure 8: Viscoelastic response of the axon when mechanically pulled
(a) Plot of cantilever position or transverse axonal displacement d vs time, (b) Plot of force response of the cantilever with time for the same case.

We have used the multiple step pull protocol to study the stress and strain response of the axon. The response plots are shown in figure 9. Here, cantilever displacement data over time is shown (figure 9A). This is same as the transverse axonal displacement and is used as an indicator of strain evolution of the axon. The plot indicates that the response of the axon over initial few steps is purely elastic, while as the step number increases, the viscous component in the response increases. Similarly, in the force response of the cantilever (figure 9B), force relaxation, which occurs due to viscous component, is seen for higher step numbers. Most live axons (n = 18/28) show this kind of nonlinear viscoelastic response. A likely mechanism for this non-linear viscoelastic behaviour, occurring when axons are subjected to increasing stress, is discussed in

later section.

a)

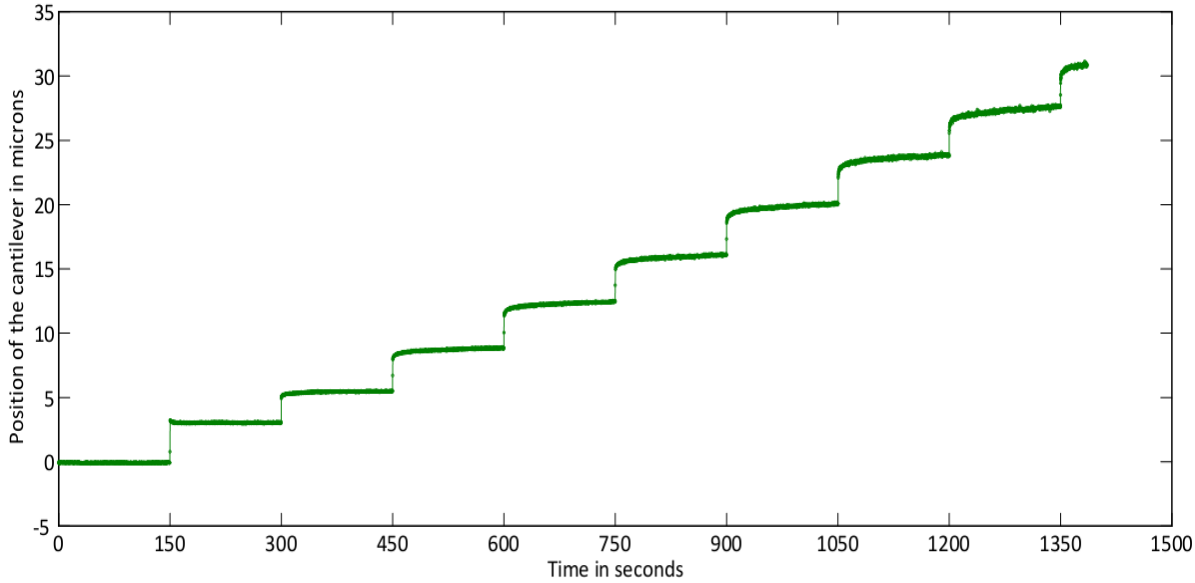

b)

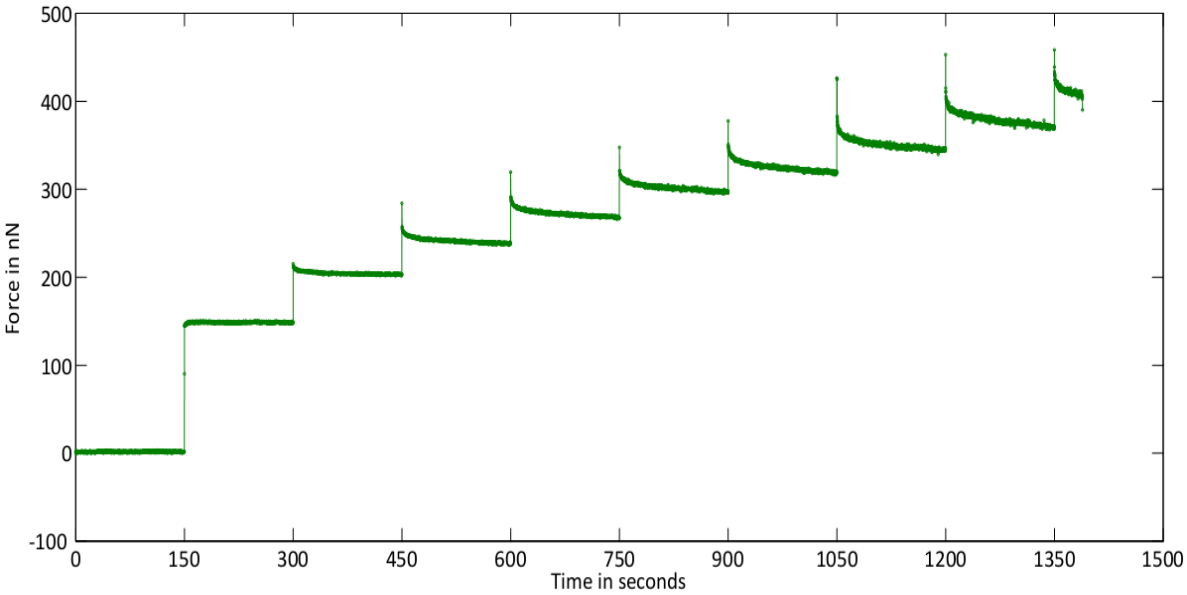

Figure 9: Nonlinear viscoelastic behaviour of an axon

This is observed in stepped pull experiment. (a) Cantilever position plot over time, (b) Force response over time

From the results of response to multiple step pull experiment, axonal tension was estimated. This was for later part of each step i.e. after viscous relaxation. Plots of this axonal tension vs axonal strain are shown in figure 10.

a)

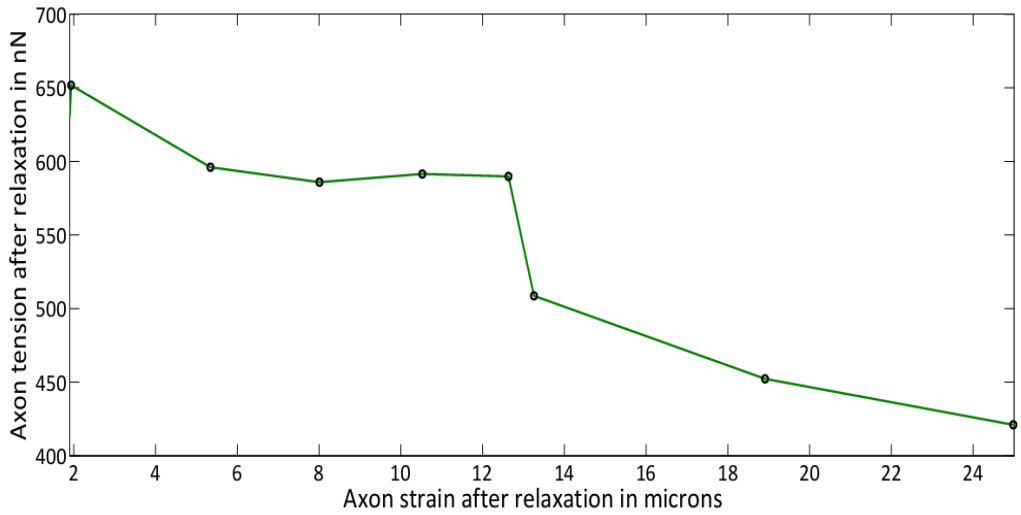

b)

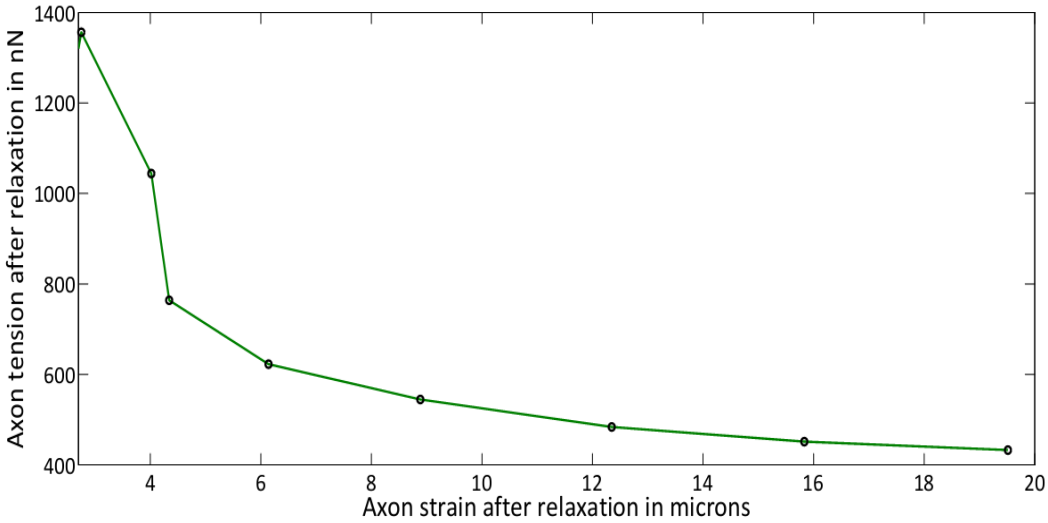

Figure 10: Axonal tension vs axonal strain

Plots for values obtained after relaxation at every step. (a) and (b) represent two such cases, for measurements on live axons.

As can be seen from these plots, axonal tension is decreasing with increasing strain in successive pulls on the axon. This is possible if the material is weakening over time, as the strain increases due to steps imposed. To test this, the net elastic constant of the axon was also plotted vs strain after relaxation for each step, as shown in figure 11. The net elastic constant is calculated using the force and strain response from the regions of the plot towards the end of each step. Assuming that towards the end of each pull, the

axon has relaxed, the elastic constant calculated using this region of the plot will be a resultant of the elastic constant of the two springs (k1 and k2) shown in the model.

a)

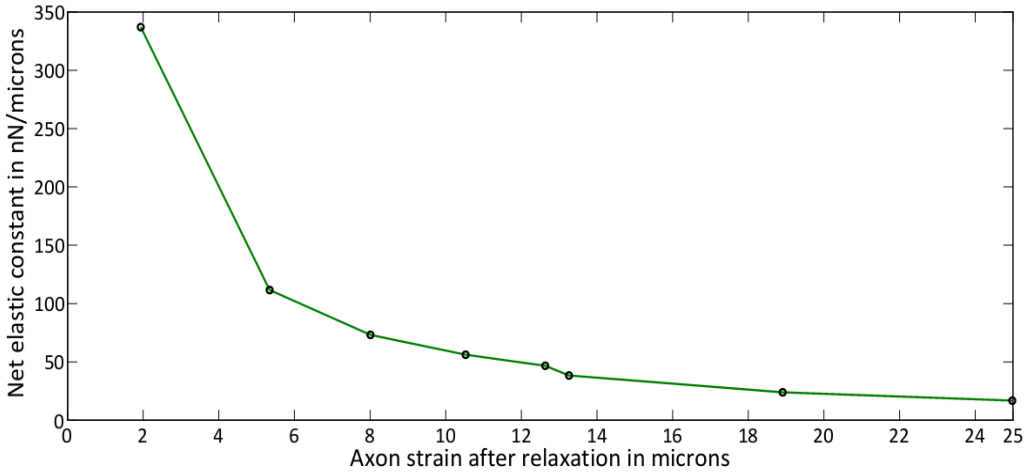

b)

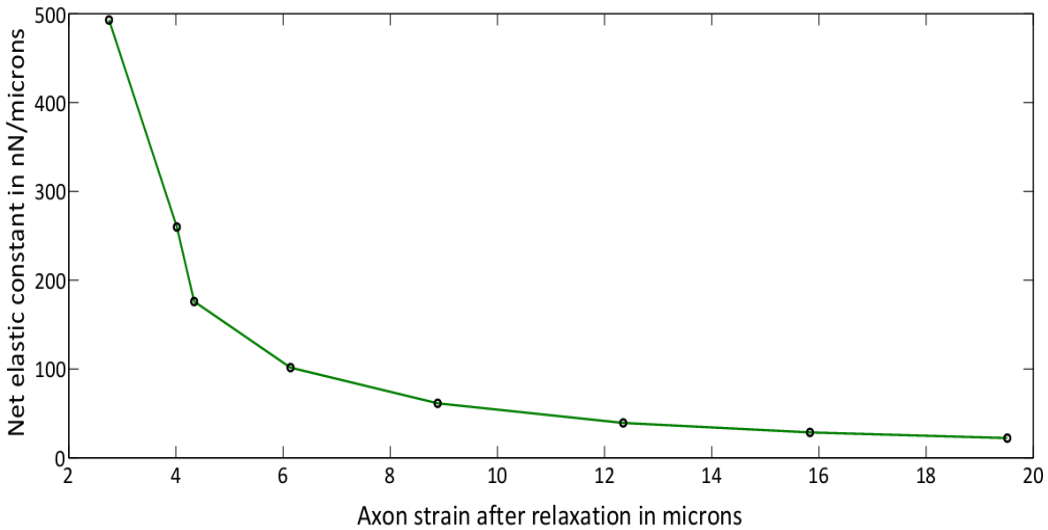

Figure 11: Net elastic constant vs axonal strain

Net elastic constant is measured for every step, from values after relaxation. (a) and (b) are the plots for the cases in figure 10a and 10b respectively .

The net elastic constant is observed to decrease with increasing strain. So, the axon is showing a weakening behaviour with increasing strain. This is in contradiction with what is usually observed about biological polymers; they show strain stiffening behaviour (Storm et al, 2005).

For the nonlinear viscoelastic behaviour observed, we hypothesized that this could be an effect of crosslinking breakage (figure 12A). The cytoskeleton of the axon, described before, is heavily cross-linked. A large range of cross-linking proteins in the axonal cytoskeleton exist, which can cross-link elements of same or different types. The attachment of these crosslinkers to the cytoskeleton is noncovalent and transient, like bonding in most biological cases. Thus at any given time, a fraction of these cross-linking proteins will be in a dissociated state i.e. not bound to the cytoskeleton. Now, upon imposing stress on such a cross-linked network, more of these bound cross-linkers may get detached. Thus, stress may have an effect on the dissociation rate of these proteins. Detachment of cross-linkers would release the energy stored in them. This stress dependent excess dissipation of energy may be the cause behind the increase in the viscous component seen in out data.

a) b)

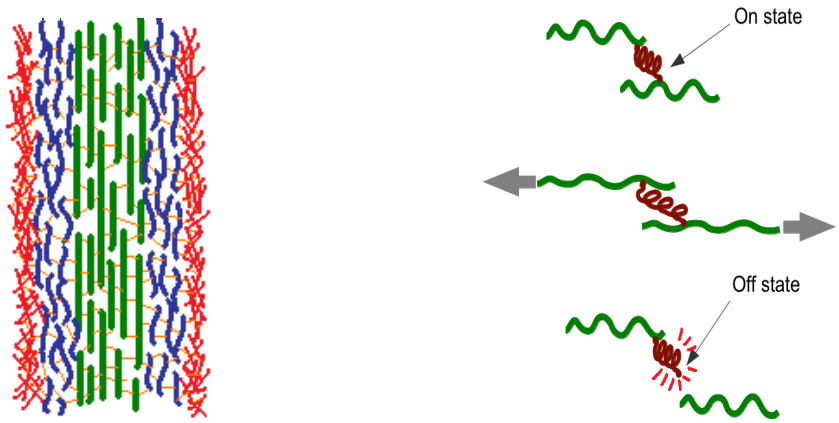

Figure 12: Hypothesis for nonlinear viscoelastic behaviour
(a) Internal structure of the axon, showing cytoskeletal cross-links. Green rods represent microtubule core, blue lines are the neurofilaments, red is the actin meshwork and the crosslinkers are shown in orange colour. (b) Crosslinker breaking upon stretch, releasing stored energy.

The observed nonlinear viscoelastic behaviour is not due to any irreversible damage caused to axons as a result of stretching. This is inferred based on some experiments conducted, where, instead of giving multiple stepped pulls, single step pulls of varying sizes were applied on axons (figure 13). Further, these pulls were also applied in a random, nonincreasing manner. Here again, for larger steps, there was an increased

viscous component in the response. The shorter pull provided following this large pull continued to show elastic response. So, the nonlinear viscoelastic behaviour is not a response to stretch induced damage or number of pulls, but a response to the stretch in the axon. Whether the response differs, when a certain deformation is reached in axon, using single steps compared to that using multiple steps remains to be systematically tested.

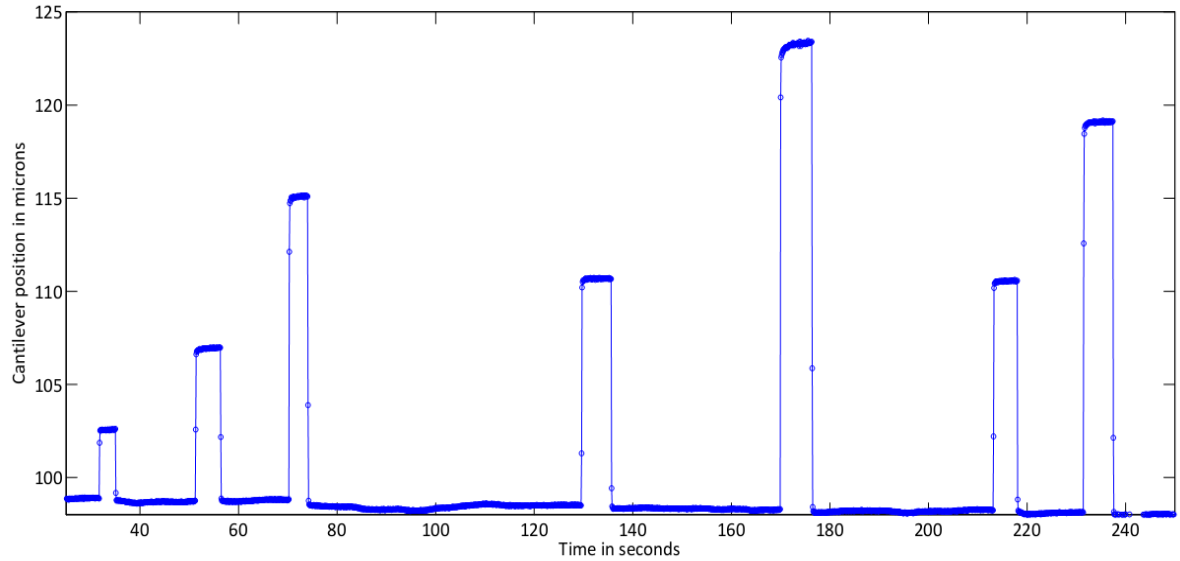

Figure 13: Experiment with single piezo steps of varying sizes. Plot shows cantilever position over time.

Crosslinkers in a network are known to modulate its mechanical properties. While cross-linking density may not have an effect on flexible polymer networks, it can affect semiflexible biopolymer networks. For eg: Gardel et al, 2004, show that actin network stiffness can change dramatically, depending on the crosslinker concentration. The network also shows stress stiffening. Gardel et al, 2006, show that in vitro actin networks cross-linked with filamin show dynamic elastic properties, similar to that of cells. Ehrlicher et al, 2011, in their study on regulation of binding of certain proteins under strain, report that filamin A, crosslinker of actin networks, allows the network to relax when stressed, by remodelling. Lieleg et al, 2008, show that thermal unbinding of crosslinks causes stress release in actin networks and increasing viscous dissipation. Lieleg et al, 2009, study the effect of transient cross-linking on the viscoelasticity of the actin network. Among other parameters, they observe a dependence of network

elasticity, and the K_{off} on the stress in the network. Viscoelastic response is shown to be governed by K_{off}, binding energy and the characteristic bond lengths of the cross-linking proteins. To show that crosslinking proteins can affect the viscoelasticity of the cytoskeleton in vivo as well, Eichinger et al, 1996 used alpha-actinin and ABP120 gelation factor mutants in *Dictyostelium*. Mutant cell viscoelasticity was indeed found to be different from that of the wild type cell.

To begin testing our hypothesis that stress dependent increase in crosslinker dissociation causes increased viscous response at higher stress, we checked if similar behaviour was also observed for fixed cells. In this case, the crosslinkers are covalently bound to the cytoskeleton. So, breaking of these covalent cross-links will now require significantly higher forces. If the hypothesis is true, one would expect nonlinear viscoelasticity to appear at forces higher than that in case of live cells, if at all. An initial comparison was done between measurements conducted on live cells vs that on fixed cells. Here, force required vs percent relative strain induced in axon is compared between live and fixed cells (figure 14).

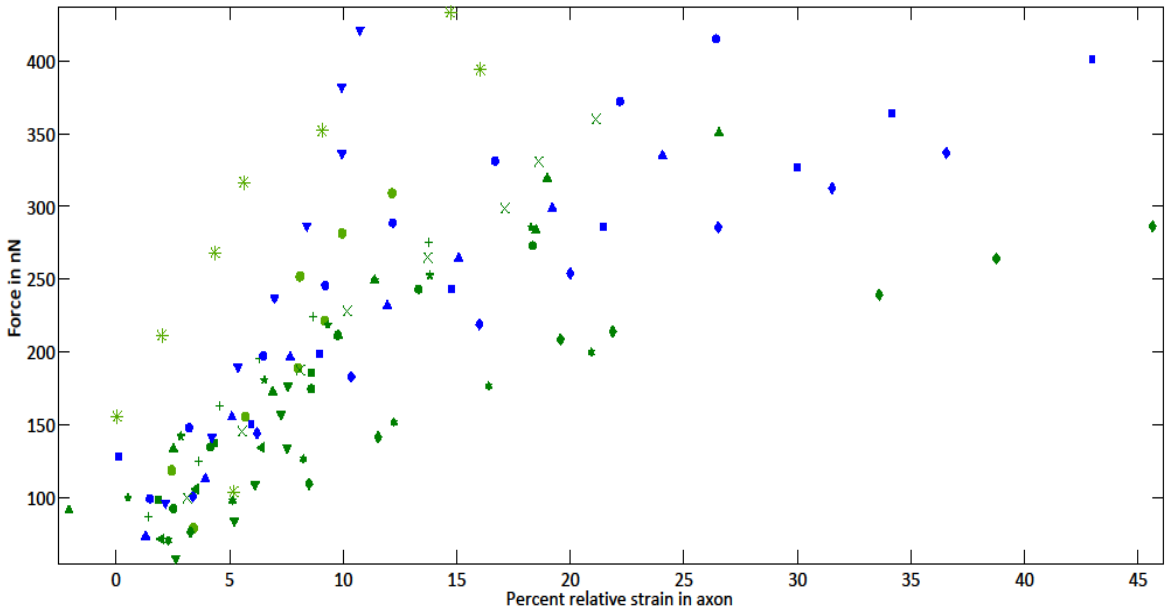

Figure 14: Bulk comparison of response of fixed and live cells.
Plot of force required vs percent relative strain induced in the axon. Points in blue are data from fixed cells, while points in green are from live cells. Different symbols indicate different axons.

It was observed that the force values for inducing certain relative amount of strain in the axon did not differ significantly between live and fixed axons. This may be a consequence of cell to cell variation in the mechanical properties. So, while individually the axons may become stiff upon fixation, when bulk comparison is done between live and fixed cells, one may not see a difference. So, we then conducted measurements on the same axon, before and after fixation. Plots below show results of one such experiment (figure 15)

a)

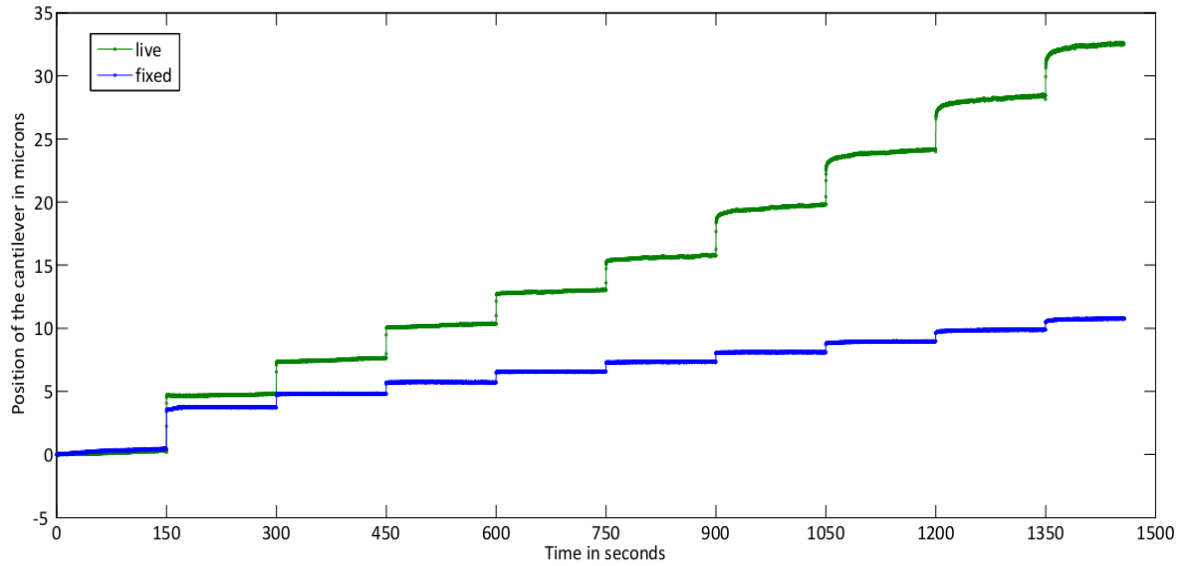

b)

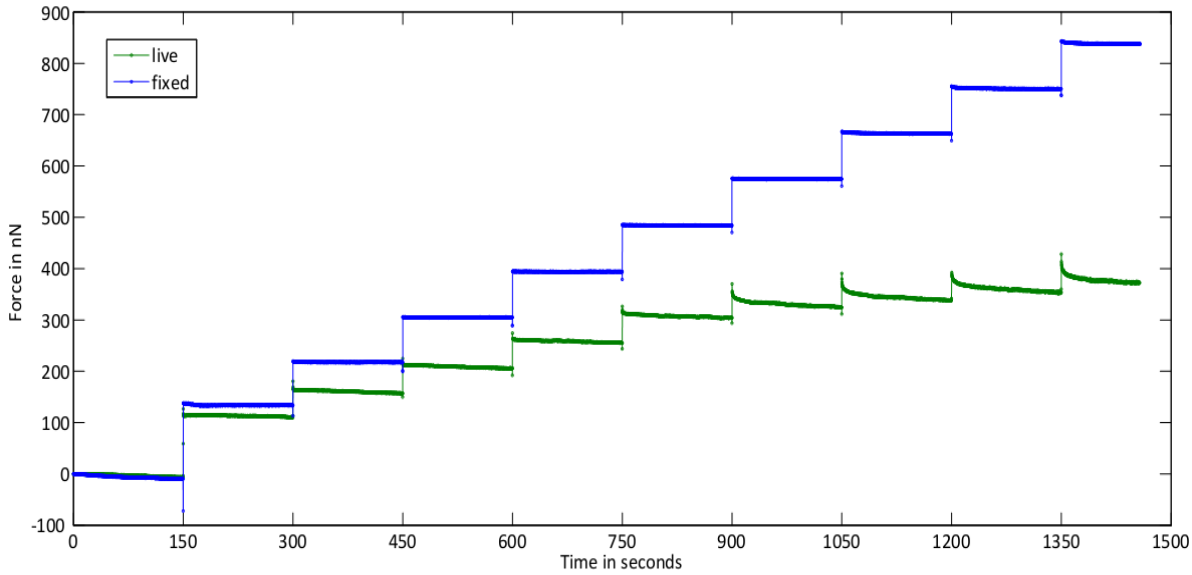

Figure 15: Comparison of single cell response, before and after fixation

Before fixation data is in green, after fixation data is in blue. (a) Cantilever position or transverse axonal displacement plotted over time, (b) Force of the cantilever vs time.

For all the axons compared in this manner (n = 6), before and after fixation, the force reached at the end of the all pulls was higher after fixation, indicating that the axon had become stiff after fixation. In cases where the nonlinear viscoelastic response was observed for live cells, the response did not occur after fixation. For eg: in the above figure, the force relaxation due to viscous component, becoming predominant after 5th pull, is not observed in the after fixation data. This result is in accordance with our hypothesis. While the model may explain the results seen for 18 of 28 live axons, we do not yet have an explanation for why the nonlinear viscoelastic effect is not seen in remaining cells.

To be able to further validate the hypothesis, a model is being developed in collaboration with Dr. Andrew-Callan Jones (unpublished, Univ. of Montpellier II). The scheme is to model the axon as a set of detachable springs. The detaching event represents cross-linking breakage, Every spring or crosslinker will have a bound state (τ_b) and unbound state (τ_u) lifetime. According to the hypothesis, stretch in the axon has an effect on crosslinker dissociation rate. This is translated as: the bound state lifetime of the spring depends on stretch in the axon. The force in the axon is then modelled as a function of probability of a spring being attached. So, if there be M springs in series and each is stretched by x,
then the total stretch in the axon = $X = Mx$.
Each of the elements in series itself consists of N springs in parallel, each of stiffness κ. These are the springs which can detach. The average force in the axon as a function of stretch X and time is then $F(X,t) = P(X,t)\,\kappa Nx = \frac{N}{M}P(X,t)\kappa X$, where P(X,t) is the probability of the spring being bound. This probability is a function of lifetimes of bound and unbound state, The spring detachment kinetics is assumed to follow Arrhenius law, which relates rate constants of reactions to temperature. Then, $\tau_b^{-1} = Ae^{E/k_BT}$. Here, A is the prefactor, which in our case is the chemical turnover rate ω_0; and the energy barrier lowering in this case is due to force in each spring = κx. The equation then

becomes: $\tau_b^{-1} = \omega_0 exp\left[\frac{\kappa x \delta}{k_B T}\right]$

This equation can be rewritten to show bound state lifetime as an exponential function of stretch in the system. Substituting for probability P(X,t) in the force equation with τ_b as an exponential function of stretch, the model predicts that force relaxation following increase in stretch will be exponential. This was checked, and the plots for the axon shown in the above case are given below (figure 16):

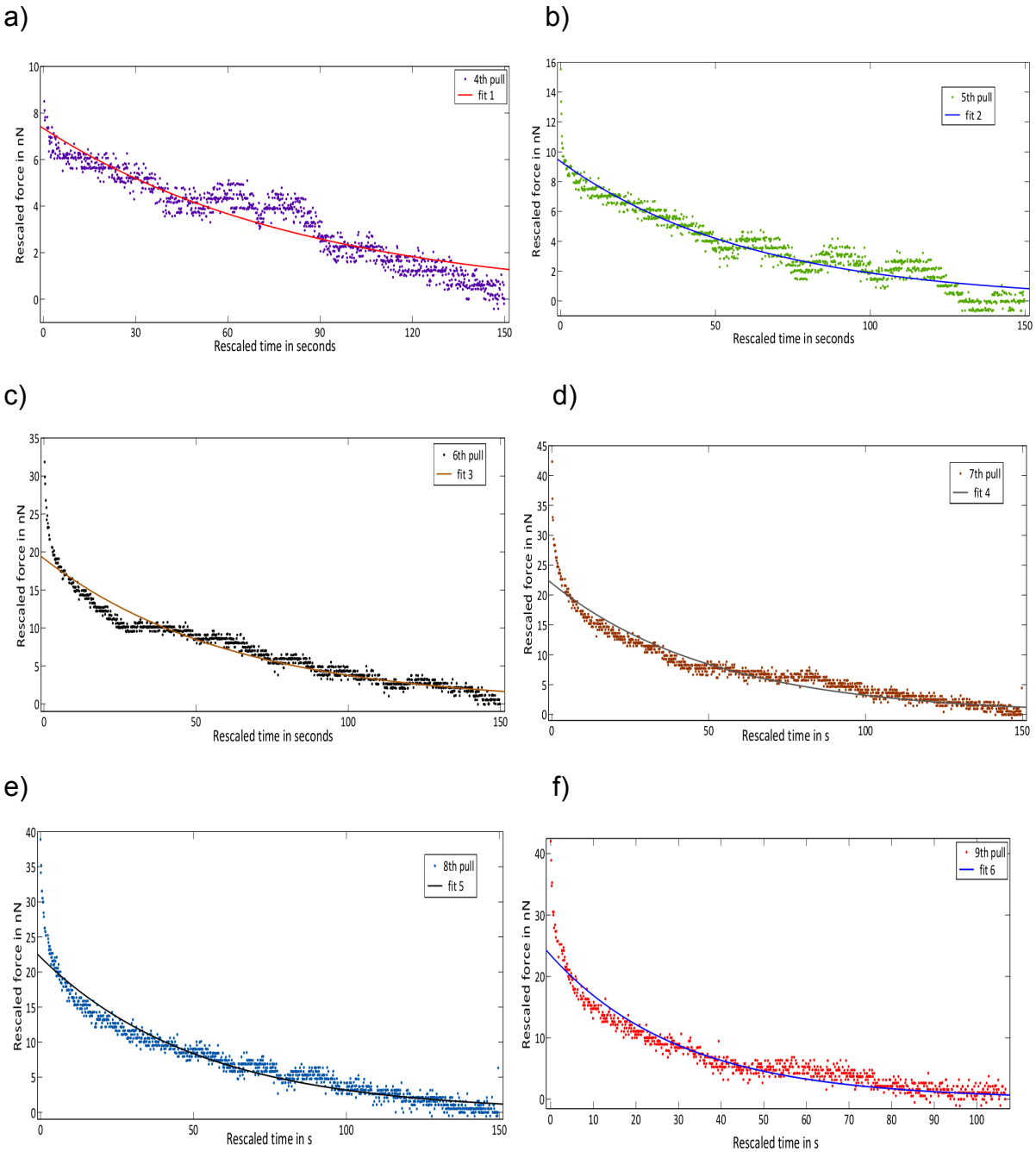

Figure 16: Exponential fits to force relaxation data for testing the model

Force relaxation vs time for measurement on live cell shown in previous fig-a, (a) for 4th

pull, (b) for 5th pull, (c) for 6th pull, (d) for 7th pull, (e) for 8th pull, (f) for 9th pull.

The equation used for exponential fitting to above plots is: $F = ae^{(bt)}$

The relaxation time = $-1/b$

The fit parameters for above cases are given in the table below:

	R-square	a	b	Relaxation time
4th pull	0.83	7.34	-0.012	86.43
5th pull	0.88	9.36	-0.016	62.38
6th pull	0.91	19.12	-0.016	61.50
7th pull	0.91	21.98	-0.019	52.08
8th pull	0.82	22.11	-0.019	51.47
9th pull	0.91	23.44	-0.033	30.50

Table 1: Fit parameters obtained from exponential fits for force relaxation data.

The exponential does not fit well to the initial rapid relaxation. This suggests existence of two or more sets of detachable springs, with varying stiffness. The softer springs would then detach rapidly, followed by the springs with higher stiffness. This is being tested.

In the future, we will be conducting similar experiments under constant force, constant strain mode. As the name suggests, here, the force or strain level will be maintained constant while the evolution of strain or stress respectively, is analyzed. This will be helpful to estimate parameters such as the elasticity and viscosity coefficients of axons, as the models for deriving these quantities usually assume one of the parameters out of stress or strain to be constant. These experiments will also be useful in testing the predictions of the model to explain nonlinear viscoelasticity in axons, described above, since the model predictions are also based on constant stress or strain assumptions.

Another interesting feature observed during these experiments was regarding the

regaining of tension by axons, upon releasing the force. In case of live cells, upon release of force at the end of the step pulls, the axon would initially go slack. Following this, within matter of a few minutes, the axon would regain its tension, inferred based on tautness of the axon. However, in case of fixed axons, this was not true. Here, following force release, the axon did not become taut again, when observed for atleast next 20 min. So, the deformation happening in this case was permanent. It would be of interest to study the mechanism of regaining of tension. The process may be based on passive mechanism. The bonds dissociated due to stress may reform upon release of stress. This would not be possible in case of fixed cells as the any bond breakage that may happen in this case would be permanent, not reversible. The change in axonal length observed during this tension regaining suggests that there is more to the process than simple reformation of bonds. The internal structure would have to rearrange to bring about length shortening. This process may be driven by active mechanisms, similar to active contractions (Dennerll et al, 1989, Bernal et al, 2007)

Another future direction for the work would be to study the cytoskeletal mechanisms behind the axonal responses to tension. The mechanisms behind all these neuronal responses to tension are not well-studied. A few experiments done in this direction for eg: include Chetta et al, 2012. Here, movement of stationary mitochondria, docked to the cytoskeleton, was observed to study the reorganization of cytoskeleton in response to stretch. Their results show that stretching had heterogenous effects along the length of the axon. Individual sections of the axon respond differently to the strain and a characteristic feature length is suggested. Another study by Kim et al, 2009 suggested a cytoskeleton based transduction mechanism, instead of stretch activated channel based, for mechanical stimulation evoked action potential. Easy coupling to fluorescence and confocal microscopy being an advantage of our system, it can be used in the future to systematically probe the roles and effects on the cytoskeletal elements. Pharmacological approaches will also aid.

To summarize, this work establishes use of the novel force apparatus for studying axonal mechanics. Mechanical step pull experiments conducted show axon to be a nonlinear viscoelastic object. In order to explain this observation, a hypothesis stating

cytoskeletal crosslinkers' dissociation dynamics to be stress dependent was proposed. Results of experiments comparing single cell responses to fixation treatment are in favour of the hypothesis. A model is being developed based on this hypothesis to generate predictions, which can be used to further test the hypothesis. Other features of the axonal response, which were analyzed, include axonal tension and net elastic constants. Their variation with strain suggest a strain weakening behaviour in stretched axons. The study begins to lay the grounds for conducting future quantitative force measurement experiments using this setup which would eventually come together to provide an integrated understanding of axonal mechanics.

4. References:

Ahmed W.W., Li T.C., Rubakhin S. S., Chiba A., Sweedler J. V., and Saif T., (2012), Mechanical tension modulates local and global vesicle dynamics in neurons, Cell Mol. Bioengg., 5, 155-164

Anava S., Greenbaum A., Ben-Jacob E., Hanein Y., and Ayali A., (2009), The regulative role of neurite mechanical tension in network development, Biophys. J., 96, 1661-1670

Avvisato C.L., Yang X., Shah S., Hoxter B., Li W., Gaynor R., Pestell R., Tozeren A., and Byers S., (2007), Mechanical force modulates global gene expression and beta-catenin signaling in colon cancer cells, J. Cell Sci., 120, 2672-2682

Bernal R., Pullarkat P., and Melo F., (2007), Mechanical properties of axons, Phys. Rev. Lett., 99,

Bernal R., Melo. F., and Pullarkat P., (2010), Drag force as a tool to test the active mechanical responses of PC12 neurites, Biophys. J., 98, 515-523

Bhadriraju K., Yang M., Ruiz S., Pirone D., Tan J., and Chen C., (2007), Exp. Cell Res., 313, 3616-3623

Bray D., (1979), Mechanical tension produced by nerve cells in tissue culture, J. Cell Sci., 37, 391-410

Bray D., (1984), Axonal growth in response to experimentally applied mechanical tension, Devel. Biol., 102, 379-389

Chada S., Lamoureux P., Buxbaum R. E., and Heidemann S. R., (1997),

Cytomechanics of neurite outgrowth from chick brain neurons, J Cell Sci., 110, 1179-1186

Chetta J., Kye C., and Shah S., (2010), Cytoskeletal dynamics in response to tensile loading of mammalian axons, Cytoskeleton, 67, 650-665

Condron B.G., and Zinn K., (1997), Regulated neurite tension as a mechanism for determination of neuronal arbor geometries in vivo, Curr. Biol., 7, 813-816

Davies P.F., and Tripathi S.C., (1993), Mechanical stress mechanisms and the cell: an endothelial paradigm, Circ. Res., 72, 239-245

Dennerll T. J., Joshi H. C., Steel V. L., Buxbaum R. E., and Heidemann S. R., (1988), Tension and compression in the cytoskeleton of PC12 neurites II: Quantitative measurements, J. Cell Biol., 107, 665-674

Dennerll T., Lamoureux P., Buxbaum R. E., and Heidemann S. R., (1989), The cytomechanics of axonal elongation and retraction, J. Cell Biol., 109, 3073-3083

Ehrlicher A. J., Nakamura F., Hartwig J. H., Weitz D. A., and Stossel T. P., (2011), Mechanical strain in actin networks regulates FilGAP and integrin binding to filamin A, Nature, 478, 260-263

Eichinger L., Koppel B., Noegel A., Schleicher M., Schliwa M., Weijer K., Witke W., and Janmey P.A, (1996), Mechanical perturbation elicits a phenotypic difference between *Dictyostelium* wild-type cells and cytoskeletal mutants, Biophys. J., 70, 1054-1060

Fass J. N., and Odde D. J., (2003), Tensile force dependent neurite elicitation via anti-beta1 integrin antibody coated magnetic beads, 85, 623-636

Franze K., Gerdelmann J., Weick M., Betz T., Pawlizak S., Lakadamyali M., Bayer J., Rillich K., Gogler M., Lu Y., Reichenbach A., Janmey P., and Kas J., (2009), Neurite branch retraction is caused by a threshold dependent mechanical impact, Biophys. J., 97, 1883-1890

Franze K., and Guck J., (2010), The biophysics of neuronal growth, Rep. Prog. Phy, 73

Gardel M.L., Shin J. H., MacKintosh F. C., Mahadevan L., Matsudaira P., Weitz D. A., (2004), Elastic behaviour of cross-linked and bundled actin networks, Science, 1301-1305

Gardel M. L., Nakamura F., Hartwig J. H., Crocker J. C., Stossel T. P., and Weitz D. A., (2006), Prestressed F-actin networks cross-linked by hinged filamins replicate

mechanical properties of cells, PNAS, 103, 1762-1767

Hanein Y., Tadmor O., Anava S., and Ayali A., (2011), Neuronal some migration is determined by neurite tension, Neurosci., 572-579

Heidemann S.R., Lamoureux P., and Buxbaum R. E., (1997), Cytomechanics of axonal development, Cell Biochem. Biophy., 27, 135-155

Hornberger T.A., and Esser K.A., (2004), Mechanotransduction and the regulation of protein synthesis in skeletal muscle, Proc. Nutrition Soc. 63, 331-335

Huang S., Chen C. S., and Ingber D. E., (1998), Control of cyclin D1, $p27^{Kip1}$, and cell cycle progression in human capillary endothelial cells by cell shape and cytoskeletal tension, Mol. Biol. of Cell, 9, 3179-3193

Huang S., and Ingber D.E., (2005), Cell tension, matrix mechanics and cancer development, Cancer Cell, 175-176

Hwang Y., Gouget C., and Barakat A., (2012), Mechanisms of cytoskeleton-mediated mechanical signal transmission in cells, Comm. Integ. Biol., 5, 538-542

Kim G. H., Kosterin P., Obaid A. L., and Salzberg B. M., (2007), A mechanical spike accompanies the action potential in mammalian nerve terminals, Biophys. J., 92, 3122-3129

Lamoureux P., Buxbaum R. E., and Heidemann S.R., (1989), Direct evidence that growth cones pull, Nature, 340, 159-162

Lamoureux P., Ruthel G., Buxbaum R. E., and Heidemann S. R., (2002), Mechanical tension can specify axonal fate in hippocampal neurons, J. Cell Biol., 159, 499-508

Lamoureux P., Heidemann S. R., Martzke N., and Miller K. E., (2009), Growth and elongation within and along the axon, Devel. Neurobiol.

Lieleg O., Claessens M. M. A. E., Luan Y., Bausch A. R., (2008), Transient binding and dissipation in cross-linked actin networks, Phys. Rev. Lett., 101

Lieleg O., Schmoller K. M., Claessens M. M. A. E., and Bausch A. R., (2009), Cytoskeletal polymer networks: viscoelastic properties are determined by the microscopic interaction potentials of cross-links, Biophys. J., 96, 4725-4732
Mammoto A., and Ingber D.E., (2009), Cytoskeletal control of growth and cell fate switching, Curr. Op. Cell Biol., 21, 864-870

Na S., Collin O., Chowdhury F., Tay B., Ouyang M., Wang Y., and Wang N., (2008), Rapid signal transduction in living cells is a unique feature of mechanotransduction, PNAS, 105, 6626-6631

Nicklas R.B., Ward S.C., and Gorbsky G.J., (1995), Kinetochore chemistry is sensitive to tension and may link mitotic forces to a cell cycle checkpoint, J. Cell Biol., 130, 929-939
Somogyi K., and Rorth P., (2004), Evidence for tension-based regulation of Drosophila MAL and SRF during invasive cell migration, Develop. cell, 7, 85-93

Paulus J. D., Willer G. B., Willer J. R., Gregg R. G., and Halloran M. C., (2009), Muscle contractions guide Rohon-Beard peripheral sensory axons, J. Neurosci., 29, 13190-13201

Pfister B., Iwata A., Meaney D., and Smith D. H., (2004), Extreme stretch growth of integrated axons, J. Neurosci., 24, 7978-7983

Pfister B., Bonislawski D. P., Smith D.H., and Cohen A., (2006), Stretch-growth axons retain the ability to transmit electrical signals, FEBS Lett., 580, 3525-3531

Rajagopalan J., Tofangchi A., and Saif T., (2010), *Drosophila* neurons actively regulate tension in vivo, Biophys. J., 99, 3208-3215
Rhee S., Jiang H., Ho C., and Grinnell F., (2007), Microtubule function in fibroblast spreading is modulated according to the tension state of cell matrix interactions, PNAS, 104, 5425-5430

Sato M., Wong T. Z., Brown D. T., and Allen R. D., (1984), Rheological properties of living cytoplasm, Cell Motility, 4, 7-23

Siechen S., Yang S., Chiba A., and Saif T., (2009), Mechanical tension contributes to clustering of neurotransmitter vesicles at presynaptic terminals, PNAS, 106, 12611-12616
Shefi O., Harel A., Chklovskii D., Ben-Jacob E., and Ayali A., (2004), Biophysical constraints on neuronal branching, Neurocomputing, 58-60, 487-495
Thompson D.W., (1917), On growth and form, Cambridge Univ. Press

Storm C., Pastore J. F., MacKintosh F. C., Lubensky T. C., and Janmey P. A., (2005), Nonlinear elasticity in biological gels, Nature, 435, 191-194

Tang-Schomer M. D., Patel A. R., Baas P.W., and Smith D. H., (2010), Mechanical breaking of microtubules in axons during dynamic stretch injury underlies delayed

elasticity, microtubule disassembly, and axon degeneration, FASEB J., 24, 1401-1410

Wang N., Tytell J., and Ingber D. E., (2009), Mechanotransduction at a distance: mechanically coupling the extracellular matrix with the nucleus, Nat. Rev. Mol. Cell Biol., 10, 75-82

Zheng J., Lamoureux P., Santiago V., Dennerll T., Buxbaum R. E., and Heidemann S. R., (1991), Tensile regulation of axonal elongation and initiation, J. Neurosci., 11, 1117-1125